


Cite this: *RSC Adv.*, 2021, **11**, 36850

## Revisiting salicylidene-based anion receptors†

Sandeep Kumar Dey,<sup>a</sup> Sonam Kumari,<sup>a</sup> Sonal Mandrekar,<sup>a</sup> Shashank N. Mhaldar,<sup>a</sup> Sarvesh S. Harmalkar<sup>a</sup> and Christoph Janiak<sup>b</sup>

Several salicylidene-based colorimetric and fluorimetric anion sensors are known in the literature. However, our <sup>1</sup>H-NMR experimental results (in DMSO-*d*<sub>6</sub>) showed hydrolysis of imine (–N=CH–) bonds in salicylidene-based receptors (SL, CL1 and CL2) in the presence of quaternary ammonium salts (*n*-Bu<sub>4</sub>N<sup>+</sup>) of halides (Cl<sup>–</sup> and Br<sup>–</sup>) and oxo-anions (H<sub>2</sub>PO<sub>4</sub><sup>–</sup>, HSO<sub>4</sub><sup>–</sup> and CH<sub>3</sub>COO<sup>–</sup>). The mono-salicylidene compound CL1 showed the most extensive –N=CH– bond hydrolysis in the presence of anions. In contrast, the di-salicylidene compound CL2 and the tris-salicylidene compound SL showed comparatively slow hydrolysis of –N=CH– bonds in the presence of anions. Anion-induced imine bond cleavage in salicylidene compounds could easily be detected in <sup>1</sup>H-NMR due to the appearance of the salicylaldehyde –CHO peak at 10.3 ppm which eventually became more intense over time, and the –N=CH– peak at 8.9–9.0 ppm became considerably weaker. Furthermore, the formation of the salicylidene O–H⋯X<sup>–</sup> (X<sup>–</sup> = Cl<sup>–</sup>/Br<sup>–</sup>) hydrogen-bonded complex, peak broadening due to proton-exchange processes and keto–enol tautomerism have also been clearly observed in the <sup>1</sup>H-NMR experiments. Control <sup>1</sup>H-NMR experiments revealed that the presence of moisture in the organic solvents could result in gradual hydrolysis of the salicylidene compounds, and the rate of hydrolysis has further been enhanced significantly in the presence of an anion. Based on <sup>1</sup>H-NMR results, we have proposed a general mechanism for the anion-induced hydrolysis of imine bonds in salicylidene-based receptors.

Received 17th October 2021  
Accepted 4th November 2021

DOI: 10.1039/d1ra07677a

rsc.li/rsc-advances

## Introduction

Schiff bases have widely been explored as chelating ligands in metal coordination chemistry for several decades,<sup>1</sup> and their metal complexes are considered to be promising candidates for a variety of applications related to catalytic activities,<sup>2</sup> photoluminescent properties<sup>3</sup> and biomedical applications.<sup>4</sup> However, with the importance of anion recognition chemistry<sup>5</sup> being increasingly recognized as an important discipline of supramolecular chemistry,<sup>6</sup> numerous salicylidene Schiff bases have been studied for anion sensing applications in the past two decades.<sup>7,8</sup> Interestingly, most salicylidene-based anion sensors are known for colorimetric detection of fluoride (F<sup>–</sup>) in aprotic solvents such as dimethyl sulfoxide (DMSO) and acetonitrile (CH<sub>3</sub>CN).<sup>7</sup> The mechanism of sensing has been attributed to either –OH⋯F<sup>–</sup> hydrogen bonding or –OH deprotonation by the fluoride ion. Some of these Schiff bases have also been reported to sense other basic anions like acetate (CH<sub>3</sub>COO<sup>–</sup>) and dihydrogenphosphate/hydrogenphosphate (H<sub>2</sub>PO<sub>4</sub><sup>–</sup> ⇌ HPO<sub>4</sub><sup>2–</sup>

+H<sup>+</sup>)<sup>9</sup> in addition to F<sup>–</sup>, depending on the choice of solvent(s).<sup>8</sup> However, no crystal structures to validate the formation of receptor–anion complexes or deprotonated receptor are reported in any of the published literature, to the best of our knowledge. Recently, we have reported that salicylidene Schiff bases are not stable in the presence of fluoride ion and undergo imine bond (–N=CH–) hydrolysis in aprotic polar media in the presence of hard-to-avoid traces of moisture (2F<sup>–</sup> + H<sub>2</sub>O ⇌ OH<sup>–</sup> + HF<sub>2</sub><sup>–</sup>) to generate deprotonated salicylaldehyde and the respective amine.<sup>10</sup> Thus, due to the apparently unavoidable imine bond hydrolysis in the presence of fluoride and water under ambient conditions,<sup>10,11</sup> it would not seem easy to obtain crystal structures of a hydrogen bonded receptor–fluoride complex or deprotonated receptor in the presence of a fluoride salt.

Anion-induced hydrolysis of –N=CH– bond was first observed by Wang and co-workers in a diketopyrrolopyrrole-derived Schiff base compound in the presence of hydrogensulfate (HSO<sub>4</sub><sup>–</sup>).<sup>12</sup> Their results are particularly important in the context of understanding the mechanism of anion sensing by Schiff bases, which may undergo hydrolysis in the presence of certain anionic species. Several chromogenic cyanide (CN<sup>–</sup>) sensors based on the nucleophilic additions of CN<sup>–</sup> to –N=CH– or O=CR– bonds are reported in the literature.<sup>13</sup> Further, numerous fluoride chemodosimeter (reactive sensors) are also known in the literature.<sup>14</sup> This suggests that the reaction between an anion and a Schiff base cannot be ruled out, and

<sup>a</sup>School of Chemical Sciences, Goa University, Taleigao Plateau, Goa 403206, India. E-mail: sandeepdey@unigoa.ac.in; Tel: +91-7387633550

<sup>b</sup>Institute of Inorganic and Structural Chemistry, Heinrich-Heine University, 40204, Düsseldorf, Germany. E-mail: janiak@uni-duesseldorf.de; Tel: +49-2118112286

† Electronic supplementary information (ESI) available: Synthesis of Schiff bases and characterization, <sup>1</sup>H-NMR experiments in the presence of *n*-Bu<sub>4</sub>N<sup>+</sup> salts. See DOI: 10.1039/d1ra07677a


detailed experimental investigations are necessary to come to a definite conclusion.

It is important to note that the anion sensing studies of the reported salicylidene-based receptors by UV-vis spectroscopy were mostly carried out with a large excess of anions (from 5 equiv. to as high as 50 equiv. of tetrabutylammonium salts) which will result in faster hydrolysis of  $-N=CH-$  bonds in comparison to the  $^1\text{H-NMR}$  experiments which were often carried out with 1–5 equivalents of tetrabutylammonium ( $n\text{-Bu}_4\text{N}^+$ ) salt added into the Schiff base solution.<sup>7,8</sup> The detailed  $^1\text{H-NMR}$  investigations have revealed the limitations of salicylidene-based receptors as anion sensors in aprotic polar media, which has not been addressed before in the literature.

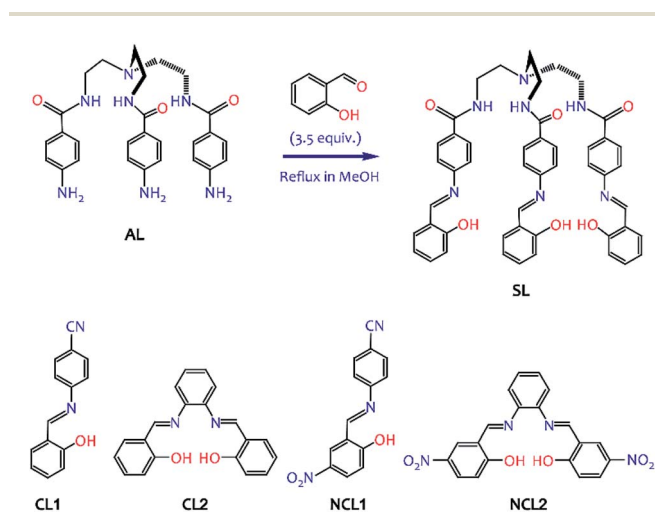
In continuation of our previous work,<sup>10</sup> herein we report the solution-state instability of salicylidene-based receptors **SL**, **CL1** and **CL2** (Scheme 1) in the presence of  $n\text{-Bu}_4\text{N}^+\text{X}^-$  ( $\text{X}^- = \text{Cl}^-$ ,  $\text{Br}^-$ ,  $\text{CH}_3\text{COO}^-$ ,  $\text{HSO}_4^-$  and  $\text{H}_2\text{PO}_4^-$ ) under non-inert conditions. Similar to the previously observed results for fluoride ion induced hydrolysis of  $-N=CH-$  bonds,<sup>10</sup> addition of other halides and oxo-anions to a solution of salicylidene Schiff base (DMSO- $d_6$ , 99.9% D atom) showed hydrogen bond formation between the salicylidene  $-OH$  and an anion, followed by keto-enol tautomerism, and eventually hydrolysis of the  $-N=CH-$  bond(s) in NMR experiments. Control experiments revealed that the addition of  $n\text{-Bu}_4\text{N}^+$  salt can significantly enhance the rate of  $-N=CH-$  bond hydrolysis in moist DMSO- $d_6$ . Based on several  $^1\text{H-NMR}$  experimental results, we propose a general mechanism for the anion-induced hydrolysis of  $-N=CH-$  bonds in salicylidene compounds.

## Results and discussions

We have recently shown the complete hydrolysis of tris-salicylidene compound **SL** (Scheme 1) in the presence of excess ( $n\text{-Bu}_4\text{N}^+\text{F}^-$  (10 equivalents)) in DMSO- $d_6$ , and also proposed a mechanism for fluoride ion induced  $-N=CH-$  bond hydrolysis under non-inert conditions.<sup>10</sup> In order to investigate

the effect of other halides and oxo-anions on  $-N=CH-$  bond hydrolysis, we have carried out  $^1\text{H-NMR}$  experiments of **SL** in the presence of 10 equiv. of ( $n\text{-Bu}_4\text{N}^+\text{Cl}^-$ , ( $n\text{-Bu}_4\text{N}^+\text{Br}^-$ , ( $n\text{-Bu}_4\text{N}^+\text{HSO}_4^-$ , ( $n\text{-Bu}_4\text{N}^+\text{H}_2\text{PO}_4^-$  and ( $n\text{-Bu}_4\text{N}^+\text{CH}_3\text{COO}^-$  in DMSO- $d_6$ .  $^1\text{H-NMR}$  spectra of **SL** mixed with either ( $n\text{-Bu}_4\text{N}^+\text{Cl}^-$ , ( $n\text{-Bu}_4\text{N}^+\text{H}_2\text{PO}_4^-$  or ( $n\text{-Bu}_4\text{N}^+\text{CH}_3\text{COO}^-$  showed gradual hydrolysis of  $-N=CH-$  bonds forming salicylaldehyde ( $\text{C}_7\text{H}_6\text{O}_2$ ) and **AL** (Scheme 1). Whereas, negligible hydrolysis of **SL** was observed in the presence of ( $n\text{-Bu}_4\text{N}^+\text{Br}^-$  and ( $n\text{-Bu}_4\text{N}^+\text{HSO}_4^-$ . In a control experiment, no hydrolysis was observed to take place for a solution of **SL** in DMSO- $d_6$ , when recorded after 5 days of sample preparation.

Addition of ( $n\text{-Bu}_4\text{N}^+\text{Cl}^-$  (10 equiv.) to a solution of **SL** in DMSO- $d_6$  did not show any notable changes in the aromatic region of the  $^1\text{H-NMR}$  spectrum of **SL**, recorded after an hour. However, the solution mixture when recorded after 24 hours (D2, Fig. 1) showed the appearance of a salicylaldehyde  $-\text{CHO}$  signal at 10.3 ppm and salicylaldehyde  $-\text{OH}$  signal at 11.3 ppm indicating the progress of  $-N=CH-$  bond hydrolysis in **SL**. Another new peak at 5.7 ppm for the  $-\text{NH}_2$  group of **AL** (Scheme 1) has also been observed, which further suggests the hydrolysis of **SL** by chloride ion. Due to hydrolysis, intensity of the  $-N=CH-$  peak at 8.9 ppm was observed to be considerably reduced with concomitant splitting of the singlet peak in the presence of chloride ion (D2, Fig. 1). The occurrence of a triplet-like peak for  $-N=CH-$  proton may be attributed to the presence of enol and keto tautomers of **SL** which are hydrogen bonded to chloride ions (Scheme 2) and appear as two closely spaced peaks in addition to the peak of free **SL**. About 27% hydrolysis was observed to be completed after 24 hours as revealed from the integral values of  $-\text{CHO}$  and  $-N=CH-$  peaks of the spectrum



**Scheme 1** Molecular structures of salicylidene Schiff bases studied here (synthesis details are provided in the ESI†).

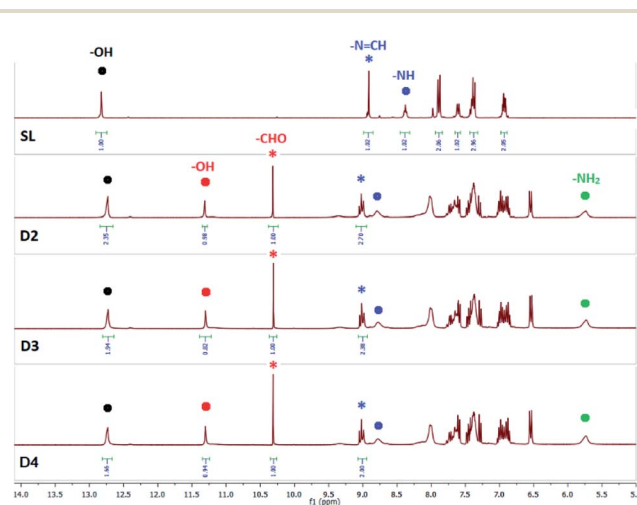
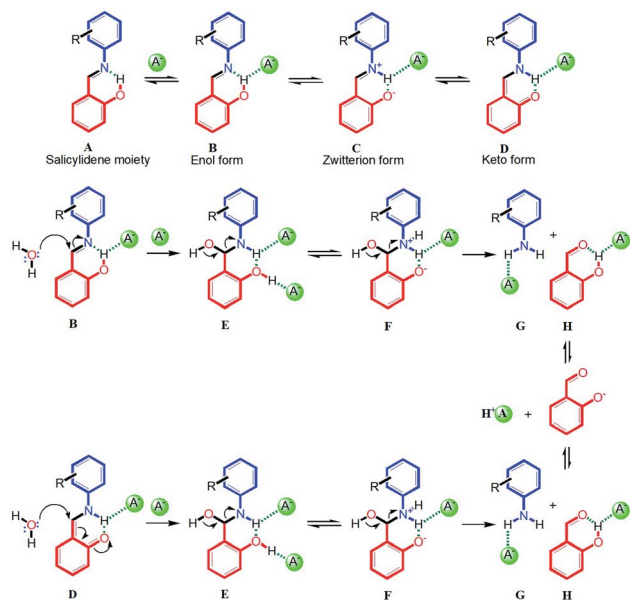


**Fig. 1** Aromatic region of  $^1\text{H-NMR}$  (DMSO- $d_6$ ) spectra of **SL** in the presence of 10 equivalents of ( $n\text{-Bu}_4\text{N}^+\text{Cl}^-$ ), recorded after 24 hours (D2), 48 hours (D3), and after 72 hours (D4). Signals labelled with red and black dots indicate  $-\text{OH}$  peaks of salicylaldehyde (red) and **SL** (black) respectively. Signals labelled with blue and green dots indicate  $-\text{NH}$  and  $-\text{NH}_2$  peaks of **SL** (blue) and **AL** (green) respectively. Signals labelled with red and blue asterisk indicate  $-\text{CHO}$  and  $-N=CH-$  protons of salicylaldehyde (red) and **SL** (blue) respectively (additional spectra are provided in the ESI†).



**Scheme 2** Plausible mechanism for the anion-induced hydrolysis of imine bond in salicylidene Schiff bases widely studied as anion sensors ( $A^- = Cl^-$ ,  $Br^-$ ,  $H_2PO_4^-$ ,  $HSO_4^-$  or  $CH_3COO^-$ ). Hydrogen bonds are shown in green dotted lines.

(D2, Fig. 1). The solution mixture when recorded on subsequent days showed further hydrolysis of **SL**, however rather slowly showing 33% hydrolysis after 72 hours (D3 and D4, Fig. 1). With hydrolysis in progress, the  $-OH$  peak of **SL** at 12.8 ppm gets broadened presumably due to the slow proton-exchange processes with moisture adsorbed by the DMSO- $d_6$  solution containing excess  $(n-Bu_4N^+)Cl^-$  (Fig. 1), both of which are hygroscopic in nature.

In contrast,  $^1H$ -NMR spectrum of **SL** mixed with  $(n-Bu_4N^+)Br^-$  (10 equiv.) in DMSO- $d_6$  did not show any hydrolysis, when recorded after 24 hours (Fig. S15, ESI $^\dagger$ ). The solution mixture when recorded after 5 days showed 3% hydrolysis of **SL** (Fig. S15 and S16, ESI $^\dagger$ ), indicating that the tripodal salicylidene-based receptor is much more stable in the presence of bromide as compared to chloride and fluoride.<sup>10</sup>

Addition of  $(n-Bu_4N^+)H_2PO_4^-$  (10 equiv.) to a solution of **SL** in DMSO- $d_6$  showed immediate disappearance of the salicylidene  $-OH$  signal at 12.8 ppm indicating fast proton-exchange processes with  $H_2PO_4^-$  ions. Further, appearance of a new peak at 10.3 ppm suggested the formation of salicylaldehyde by  $-N=CH-$  bond hydrolysis (D1, Fig. 2). However, the salicylaldehyde  $-OH$  peak at 11.3 ppm (observed in the presence of  $Cl^-$  in Fig. 1) has not been observed here, further suggests proton-exchange between  $H_2PO_4^-$  ions and phenolic  $-OH$  groups. The solution mixture when recorded after 24 hours (D2, Fig. 2) showed 44% hydrolysis of **SL** as revealed from the integral values of  $-CHO$  and  $-N=CH-$  peaks of the spectrum. Negligible hydrolysis was observed to take place in the same sample analysed on the subsequent days (D4, Fig. 2). The  $-NH_2$  peak of **AL** has experienced broadening and appeared downfield shifted at around 8.0 ppm (observed at 5.7 ppm in the presence of  $Cl^-$ ) likely due to strong hydrogen bond interactions with

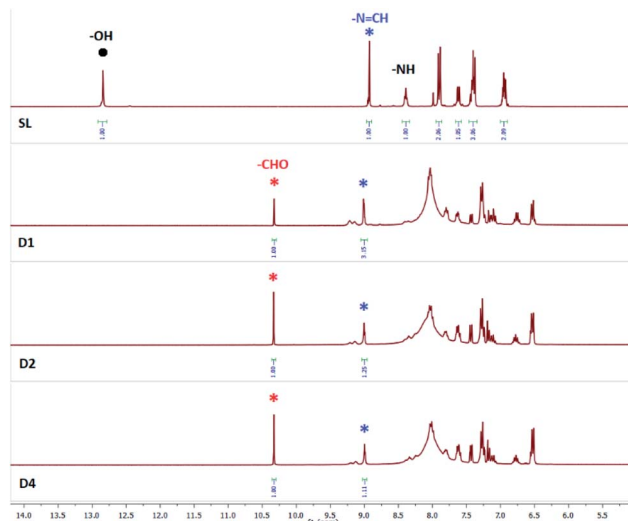


**Fig. 2** Aromatic region of  $^1H$ -NMR (DMSO- $d_6$ ) spectra of **SL** in the presence of 10 equivalents of  $(n-Bu_4N^+)H_2PO_4^-$ , recorded after 1 hour (D1), 24 hours (D2) and after 72 hours (D4). Signals labelled with red and blue asterisk indicate  $-CHO$  and  $-N=CH-$  protons of salicylaldehyde (red) and **SL** (blue) respectively. Signal labelled with black dot represent  $-OH$  proton of **SL** (additional spectra are provided in the ESI $^\dagger$ ).

$H_2PO_4^-$  ions.<sup>15</sup> In a control experiment, addition of one equivalent of  $(n-Bu_4N^+)H_2PO_4^-$  to a solution of **AL** in DMSO- $d_6$  resulted in broadening of  $-NH_2$  signal (Fig. S40, ESI $^\dagger$ ). Broadening of  $-NH_2$  signal of **AL** (at 5.7 ppm) has also been observed in the presence of one equivalent of  $(n-Bu_4N^+)Cl^-$  (Fig. S41, ESI $^\dagger$ ).

Addition of  $(n-Bu_4N^+)HSO_4^-$  (10 equiv.) to a solution of **SL** in DMSO- $d_6$  also showed immediate disappearance of the  $-OH$  signal due to fast proton-exchange processes. However, hydrolysis was observed to be very slow as compared to  $H_2PO_4^-$  and the appearance of salicylaldehyde  $-CHO$  peak at 10.3 ppm could hardly be observed even after 24 hours. Only 13% hydrolysis of **SL** was observed to be completed after 5 days, beyond which no further hydrolysis was observed (Fig. S17 and S18, ESI $^\dagger$ ).

A solution of **SL** and  $(n-Bu_4N^+)CH_3COO^-$  (10 equiv.) in DMSO- $d_6$  when recorded after one hour showed appearance of a salicylaldehyde  $-CHO$  signal and disappearance of the salicylidene  $-OH$  signal (D1, Fig. 3). The solution mixture showed 33% hydrolysis of **SL** after 48 hours beyond which no further hydrolysis was observed (D3, Fig. 3). The  $-N=CH-$  singlet (at 8.9 ppm) has split into two closely spaced signals suggesting the presence of both enol and keto forms of **SL** (Fig. 3). Similar splitting of  $-N=CH-$  singlet has also been observed for the solution **SL** mixed with  $(n-Bu_4N^+)H_2PO_4^-$  (Fig. 2).

Thus, the salicylidene-based tripodal receptor **SL** is largely stable in the presence of excess  $Br^-$  and  $HSO_4^-$  as compared to  $Cl^-$ ,  $CH_3COO^-$  and  $H_2PO_4^-$ . Since, no significant hydrolysis of **SL** has been observed after 48 hours in the presence of  $Cl^-$ ,  $CH_3COO^-$  and  $H_2PO_4^-$  (Table S1, ESI $^\dagger$ ) the equilibrium constant has been calculated considering the concentrations of **SL** and hydrolysis products (**AL** and salicylaldehyde) after 72



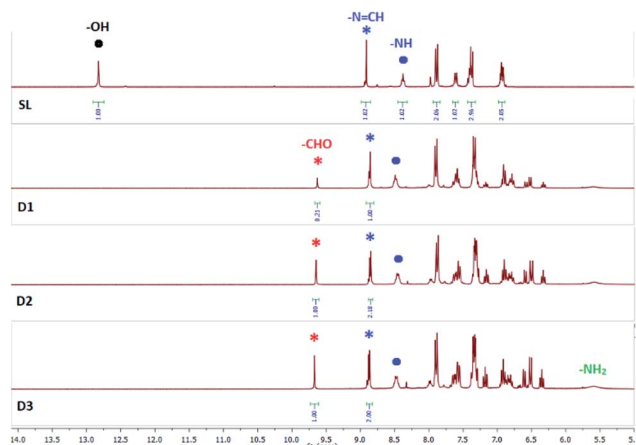


Fig. 3 Aromatic region of  $^1\text{H}$ -NMR ( $\text{DMSO}-d_6$ ) spectra of **SL** in the presence of 10 equivalents of  $(n\text{-Bu}_4\text{N}^+)\text{CH}_3\text{COO}^-$ , recorded after 1 hour (D1), 24 hours (D2) and after 48 hours (D3). Signals labelled with red and blue asterisk indicate  $-\text{CHO}$  and  $-\text{N}=\text{CH}-$  protons of salicylaldehyde (red) and **SL** (blue) respectively. Signals labelled with black and blue dots indicate  $-\text{OH}$  and  $-\text{NH}$  peaks of **SL** (additional spectra are provided in the ESI†).

hours. The equilibrium constant ( $K$ ) for the hydrolysis of **SL** in the presence of different tetrabutylammonium salts is expressed by the equation  $K[\text{H}_2\text{O}]^3 = [\text{AL}] \times [\text{C}_7\text{H}_6\text{O}_2]^3/[\text{SL}]$  ( $\text{mol}^3 \text{L}^{-3}$ ), since the water peak could not be observed distinctly in several of the  $^1\text{H}$ -NMR experiments ( $\text{DMSO}-d_6$ ) of **SL** mixed with a tetrabutylammonium salt. We believe that this includes the concentration of water in the calculation of  $K$ , so that the  $K$  values for a salicylidene compound will reflect a conclusive comparison for different anions under identical experimental conditions. Thus,  $K[\text{H}_2\text{O}]^3$  for the solution mixtures of **SL** with  $\text{Cl}^-$ ,  $\text{CH}_3\text{COO}^-$  and  $\text{H}_2\text{PO}_4^-$  (10 equiv.) were calculated to be  $2.411 \times 10^{-5}$ ,  $3.115 \times 10^{-5}$  and  $1.262 \times 10^{-4} \text{ mol}^3 \text{L}^{-3}$ , respectively (Table S3, ESI†).

Anion-induced hydrolysis of imine bond was also observed in the mono-salicylidene compound **CL1** (Scheme 1). In a control experiment, no hydrolysis was observed to take place for a solution of **CL1** in  $\text{DMSO}-d_6$ , when recorded after 5 days of sample preparation. Similar mono-salicylidene Schiff bases have previously been reported as colorimetric fluoride sensors in aprotic solvent media under ambient conditions.<sup>7a-d,8a-i</sup>  $^1\text{H}$ -NMR experiments revealed that a solution of **CL1** mixed with  $(n\text{-Bu}_4\text{N}^+)\text{Cl}^-$  (5 equiv.) in  $\text{DMSO}-d_6$  showed 84% hydrolysis after 24 hours (Fig. 4a and b), as calculated from the integral values of the salicylaldehyde  $-\text{CHO}$  peak (10.3 ppm) and the imine  $-\text{N}=\text{CH}-$  peak (9.0 ppm). The salicylaldehyde  $-\text{OH}$  peak appeared at 11.3 ppm whereas, the salicylidene  $-\text{OH}$  peak at 12.5 ppm has disappeared in the presence of excess chloride ions.

Unlike the tris-salicylidene compound **SL** which showed negligible hydrolysis in the presence of bromide ions, a solution of **CL1** mixed with  $(n\text{-Bu}_4\text{N}^+)\text{Br}^-$  (5 equiv.) in  $\text{DMSO}-d_6$  showed 70% hydrolysis after 5 days (Fig. S23, ESI†). Similarly, **CL1** in the presence of  $(n\text{-Bu}_4\text{N}^+)\text{HSO}_4^-$  (5 equiv.) showed 75% hydrolysis in  $\text{DMSO}-d_6$  after 5 days (Fig. S24, ESI†). Notably, the  $-\text{NH}_2$  peak

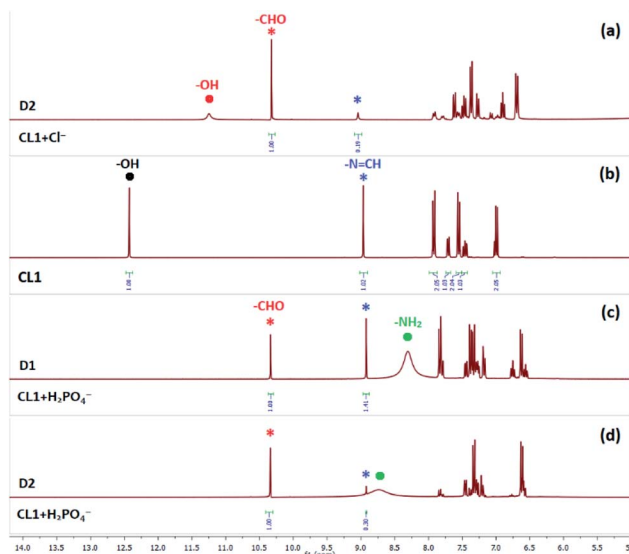


Fig. 4 Aromatic region of  $^1\text{H}$ -NMR ( $\text{DMSO}-d_6$ ) spectra of **CL1** in the presence of 5 equivalents of  $(n\text{-Bu}_4\text{N}^+)\text{Cl}^-$  and  $(n\text{-Bu}_4\text{N}^+)\text{H}_2\text{PO}_4^-$  recorded after 1 hour (D1) and after 24 hours (D2). Signals labelled with red and blue asterisk indicate  $-\text{CHO}$  and  $-\text{N}=\text{CH}-$  protons of salicylaldehyde (red) and **CL1** (blue) respectively. Signals labelled with red and black dots indicate  $-\text{OH}$  peaks of salicylaldehyde (red) and **CL1** (black) respectively (additional spectra are provided in the ESI†).

of 4-aminobenzonitrile (hydrolysis product) has experienced broadening in the presence of hydrogensulfate, but appeared as a sharp peak at 6.3 ppm in the presence of bromide (Fig. S25, ESI†). However, the  $-\text{NH}_2$  peak of 4-aminobenzonitrile was not observed in the presence of chloride possibly due to significant peak broadening. Strong hydrogen bonds between  $-\text{NH}$  protons and anions often lead to peak broadening with shifts in  $^1\text{H}$ -NMR signals, which is a case of dynamic anion coordination *i.e.*, the exchange of complexed and un-complexed guest (anion) is within the NMR time scale.<sup>15</sup>

Similar to the spectral changes of **SL** (Fig. 2), addition of  $(n\text{-Bu}_4\text{N}^+)\text{H}_2\text{PO}_4^-$  (5 equiv.) to a solution of **CL1** in  $\text{DMSO}-d_6$  resulted in the disappearance of the  $-\text{OH}$  signal at 12.5 ppm and appearance of the salicylaldehyde  $-\text{CHO}$  signal at 10.3 ppm (Fig. 4b and c). The broad peak at 8–8.5 ppm can be assigned to the  $-\text{NH}_2$  group of 4-aminobenzonitrile (a hydrolysis product) which was observed at 6.3 ppm in the presence of  $(n\text{-Bu}_4\text{N}^+)\text{Br}^-$ . The significant downfield shift of the  $-\text{NH}_2$  peak with concomitant broadening is an indication towards strong hydrogen bonding between  $-\text{NH}_2$  group and  $\text{H}_2\text{PO}_4^-$  ions. The  $-\text{NH}_2$  peak has experienced further downfield shift with time and the  $-\text{N}=\text{CH}-$  peak at 8.9 ppm has partly merged with the broad  $-\text{NH}_2$  peak after 24 hours (Fig. 4d). Thus, the percentage of hydrolysis could not be determined accurately from the spectrum recorded after 24 hours, and roughly 75% hydrolysis of **CL1** was calculated from the integral values of  $-\text{CHO}$  (10.3 ppm) and  $-\text{N}=\text{CH}-$  (8.9 ppm) peaks (Fig. 4d). In order to accurately estimate the percentage of hydrolysis, the  $^1\text{H}$ -NMR analysis of a  $\text{DMSO}-d_6$  solution of **CL1** and  $(n\text{-Bu}_4\text{N}^+)\text{H}_2\text{PO}_4^-$  (5 equiv.) were carried out every hour. With hydrolysis in





progress, the broad  $\text{-NH}_2$  peak was observed to shift downfield and begin to merge with the  $\text{-N=CH-}$  peak after 2 hours. Peak integral values showed 50% hydrolysis of **CL1** after an hour and roughly 75% hydrolysis was completed after 5 hours suggesting that no further hydrolysis has occurred after 5 hours (Fig. S51, ESI†). In a control experiment, addition of less than one equivalent of  $(n\text{-Bu}_4\text{N}^+)\text{H}_2\text{PO}_4^-$  to a solution of 4-aminobenzonitrile showed downfield shift of the broad  $\text{-NH}_2$  peak from 4.0 ppm to 6.2 ppm suggesting hydrogen bonding interactions of  $\text{-NH}_2$  group with the oxo-anion (Fig. S42, ESI†).

Addition of  $(n\text{-Bu}_4\text{N}^+)\text{CH}_3\text{COO}^-$  (5 equiv.) to a solution of **CL1** in  $\text{DMSO-d}_6$  showed 30% hydrolysis after an hour and complete hydrolysis was observed when the solution mixture was recorded after 48 hours (Fig. S26 and S27, ESI†). The  $\text{-NH}_2$  peak of 4-aminobenzonitrile appeared as a broad signal at 5.2 ppm and the salicylaldehyde  $\text{-CHO}$  peak appeared at 10.3 ppm.

Salicylidene-based receptor **CL2** has previously been reported as a colorimetric fluoride sensor in  $\text{DMSO}$ .<sup>7e</sup> In our experiments, a  $\text{DMSO-d}_6$  solution of **CL2** mixed with  $(n\text{-Bu}_4\text{N}^+)\text{Cl}^-$  (5 equiv.) showed progressive hydrolysis of  $\text{-N=CH-}$  bond as evident from the appearance of a salicylaldehyde  $\text{-CHO}$  peak at 10.3 ppm and a salicylaldehyde  $\text{-OH}$  peak at 11.3 ppm in the  $^1\text{H-NMR}$  spectrum (D2, Fig. 5). Further, the  $\text{-NH}_2$  peak at 5.4 ppm could also be observed for the corresponding amine product confirming hydrolysis of **CL2**. The  $\text{-OH}$  signal of **CL2** appearing at 13.0 ppm became significantly weaker and broad in the presence of chloride indicative of slow proton-exchange processes with moisture adsorbed by the  $\text{DMSO-d}_6$  solution

containing  $(n\text{-Bu}_4\text{N}^+)\text{Cl}^-$ . The  $\text{-N=CH-}$  singlet at 9.0 ppm (**CL2** in Fig. 5) has split into two distinct peaks occurring at 8.9 and 9.0 ppm (D2, Fig. 5) due to partial tautomerization of the enol (**e**) form to the keto (**k**) form of **CL2** (Scheme 2). In addition to the hydrolysis products, the presence of hydrogen bonded adducts formed between the  $\text{-OH}$  groups of **CL2** and  $\text{Cl}^-$  could also be observed in the  $^1\text{H-NMR}$  spectra (Fig. 5). Two new peaks corresponding to two different types of hydrogen bonded  $\text{O-H}\cdots\text{Cl}^-$  adducts appeared at 10.35 and 12.35 ppm. Due to the presence of two types of hydrogen bonded adducts in solution, two additional peaks have also appeared for the imine  $\text{-N=CH-}$  proton at 8.4 and 10.0 ppm, each of which splits into two distinct peaks due to keto-enol tautomerism. The  $\text{-N=CH-}$  peaks at 8.9(**k**)/9.0(**e**) ppm are associated with free **CL2**. Identical  $\text{-N=CH-}$  peaks observed at 8.4(**k**)/8.5(**e**) and 9.9(**k**)/10(**e**) ppm correspond to the  $\text{O-H}\cdots\text{Cl}^-$  hydrogen bonded signals at 10.35 and 12.35 ppm, respectively (D2, Fig. 5).

The solution mixture when recorded after 72 hours (D4, Fig. 5) showed complete disappearance of the salicylidene  $\text{-OH}$  signal at 13.0 ppm and intensity of the  $\text{-N=CH-}$  peaks at 8.9(**k**)/9.0(**e**) ppm was significantly quenched. Peak broadening of the hydrogen bonded  $\text{O-H}\cdots\text{Cl}^-$  signal at 12.35 ppm was also observed. However, no change in peak intensity and integral values were observed for the  $\text{-N=CH-}$  peaks at 8.4(**k**)/8.5(**e**) ppm and the corresponding hydrogen bonded  $\text{-OH}$  signal at 10.35 ppm that appears partially merged with the  $\text{-CHO}$  peak. The extent of hydrolysis could not be determined accurately due to the presence of multiple species in the solution containing **CL2** and  $(n\text{-Bu}_4\text{N}^+)\text{Cl}^-$  (D2 and D4, Fig. 5). Due to the weaker basicity and lower hydration enthalpy of  $\text{Cl}^-$ , free  $\text{-OH}$  peaks and hydrogen bonded  $\text{-OH}$  peaks of **CL2** could be observed in the presence of  $\text{Cl}^-$ , which were not observed in the presence of more basic anions ( $\text{F}^-$  and  $\text{CO}_3^{2-}$ ).<sup>10</sup>

Similar spectral changes have also been observed for a solution of **CL2** mixed with  $(n\text{-Bu}_4\text{N}^+)\text{Br}^-$  (5 equiv.) in  $\text{DMSO-d}_6$ . The solution mixture when recorded after 5 days showed the presence of a salicylaldehyde  $\text{-CHO}$  peak, an amine  $\text{-NH}_2$  peak and three distinct peaks for the  $\text{-N=CH-}$  proton, each of which splits into two distinct signals due to keto-enol tautomerism. The peak at 9.0 ppm corresponds to  $\text{-N=CH-}$  of free **CL2**, and two additional peaks observed at 8.9 and 8.2 ppm represent  $\text{-N=CH-}$  of two different hydrogen bonded  $\text{O-H}\cdots\text{Br}^-$  adducts of **CL2** (Fig. S36, ESI†). Peak integral values of the  $\text{-CHO}$  and three  $\text{-N=CH-}$  signals showed roughly 20% hydrolysis after 5 days. However, in a control experiment, no hydrolysis was observed to take place for a solution of **CL2** in  $\text{DMSO-d}_6$ , when recorded after 5 days of sample preparation.

A solution of **CL2** and  $(n\text{-Bu}_4\text{N}^+)\text{HSO}_4^-$  (5 equiv.) in  $\text{DMSO-d}_6$  showed only 12% hydrolysis after 5 days. The salicylidene  $\text{-OH}$  peak was observed to be broadened due to proton-exchange with  $\text{HSO}_4^-$ , while the  $\text{-CHO}$  and  $\text{-NH}_2$  peaks of hydrolysis products could distinctly be observed at 10.3 and 5.4 ppm suggesting slow hydrolysis (Fig. S37, ESI†). Three distinct signals for the  $\text{-N=CH-}$  proton (at 9.0, 8.9 and 8.2 ppm) has also been observed in this case.

Addition of  $(n\text{-Bu}_4\text{N}^+)\text{H}_2\text{PO}_4^-$  (5 equiv.) to a solution of **CL2** in  $\text{DMSO-d}_6$  showed disappearance of the  $\text{-OH}$  peak at 13.0 ppm

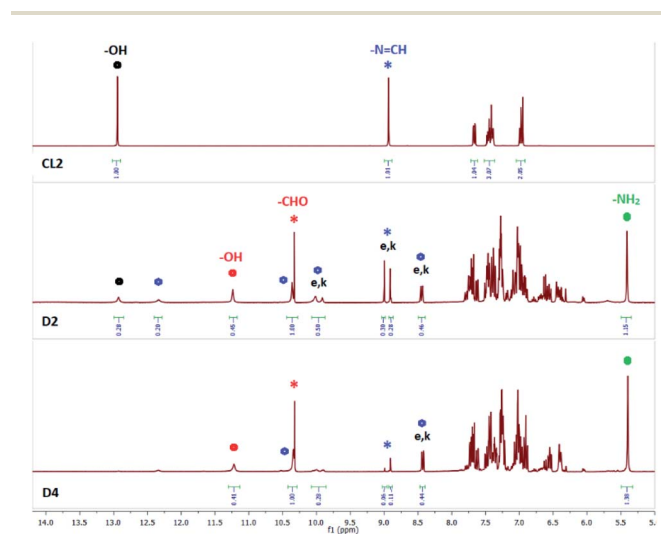


Fig. 5 Aromatic region of  $^1\text{H-NMR}$  spectra ( $\text{DMSO-d}_6$ ) of **CL2** in the presence of 5 equivalents of  $(n\text{-Bu}_4\text{N}^+)\text{Cl}^-$ , recorded after 24 hours (D2) and after 72 hours (D4). Signals labelled with **e** and **k** indicate the enol and keto forms of **CL2** respectively. Signals labelled with red and blue asterisk indicate  $\text{-CHO}$  and  $\text{-N=CH-}$  protons of salicylaldehyde (red) and **CL2** (blue) respectively. Signals labelled with blue hexagons represent  $\text{-OH}$  signals for  $\text{O-H}\cdots\text{Cl}^-$  hydrogen bonded complexes and the corresponding keto-enol peaks for the H-bond complexes. Signals labelled with red and black dots indicates  $\text{-OH}$  peaks of salicylaldehyde (red) and **CL2** (black) respectively (additional spectra are provided in the ESI†).



and appearance of the salicylaldehyde  $-CHO$  peak at 10.3 ppm (D2, Fig. 6), similar to the observed spectral changes of **SL** and **CL1** in the presence of  $(n\text{-Bu}_4\text{N}^+)\text{H}_2\text{PO}_4^-$  (Fig. 2 and 4). Further, the  $-N=CH-$  peak at 9.0 ppm (**CL2** in Fig. 6) has split into two distinct signals occurring at 8.9 and 9.0 ppm (D2, Fig. 6) due to the presence of keto (**k**) and enol (**e**) forms of **CL2**, which was also observed in the presence of  $(n\text{-Bu}_4\text{N}^+)\text{Cl}^-$ . The enol form is present in greater proportion as compared to the keto form. The solution mixture when recorded after 48 hours showed further hydrolysis and a broad peak at 8.0–8.5 ppm was observed for the  $-NH_2$  group of regenerated amine. The  $-NH_2$  signal appeared as a sharp and intense peak at 5.4 ppm for **CL2** mixed with either  $(n\text{-Bu}_4\text{N}^+)\text{Cl}^-$  or  $(n\text{-Bu}_4\text{N}^+)\text{Br}^-$ , but in the presence of  $(n\text{-Bu}_4\text{N}^+)\text{H}_2\text{PO}_4^-$ , the  $-NH_2$  signal appeared broad and much more downfield shifted likely due to the strong hydrogen bonding interactions between  $-NH_2$  group and  $\text{H}_2\text{PO}_4^-$  ions (basicity of  $\text{H}_2\text{PO}_4^- > \text{Cl}^-$ ).<sup>15</sup> About 25% hydrolysis was observed to be completed after 72 hours (D4, Fig. 6).

Although keto and enol tautomer peaks could clearly be observed in the spectrum of **CL2** mixed with an excess of  $(n\text{-Bu}_4\text{N}^+)\text{X}^-$  in  $\text{DMSO-d}_6$ , yet we have carried out variable temperature  $^1\text{H-NMR}$  analysis of a solution of **CL2** and  $(n\text{-Bu}_4\text{N}^+)\text{H}_2\text{PO}_4^-$  in  $\text{CDCl}_3$  with the objective to better understand the anion-induced hydrolysis mechanism of salicylidene Schiff bases. However, no additional information could be extracted from the spectra of the solution mixture recorded at room temperature,  $0^\circ\text{C}$  and at  $-20^\circ\text{C}$ . No splitting of the imine  $-N=$

$\text{CH-}$  peak (8.62 ppm) was observed at room temperature and at  $0^\circ\text{C}$  after 1 hour and 6 hours of sample preparation in  $\text{CDCl}_3$  (Fig. S52 and S53, ESI†). In contrast, the spectra obtained at  $-20^\circ\text{C}$  showed minor splitting and broadening of the  $-N=CH-$  peak, which is less prominent in comparison to the well separated sharp peaks of keto and enol forms observed in the spectra recorded in  $\text{DMSO-d}_6$ .

Addition of  $(n\text{-Bu}_4\text{N}^+)\text{CH}_3\text{COO}^-$  (5 equiv.) to a solution of **CL2** in  $\text{DMSO-d}_6$  showed only 10% hydrolysis after an hour and about 35% hydrolysis was observed to be completed after 48 hours (Fig. S34 and S35, ESI†). Disappearance of the salicylidene  $-OH$  peak, appearance of the  $-CHO$  peak and splitting of the  $-N=CH-$  peak into two closely spaced signals has also been observed here.

The equilibrium constant ( $K$ ) for the hydrolysis of **CL2** in the presence of  $(n\text{-Bu}_4\text{N}^+)\text{H}_2\text{PO}_4^-$  and  $(n\text{-Bu}_4\text{N}^+)\text{CH}_3\text{COO}^-$  are expressed by the equation  $K[\text{H}_2\text{O}] = [\text{APIP}] \times [\text{C}_7\text{H}_6\text{O}_2]/[\text{CL2}] \text{ mol L}^{-1}$  ( $\text{APIP} = 2\text{-aminophenyl iminophenol}$ , hydrolysis product), since the water peak could not be observed in several of the  $^1\text{H-NMR}$  experiments ( $\text{DMSO-d}_6$ ) of **CL2** and hence, the concentration of water could not be determined from some of the spectra. Thus,  $K[\text{H}_2\text{O}]$  for the solution mixtures of **CL2** with  $\text{CH}_3\text{COO}^-$  and  $\text{H}_2\text{PO}_4^-$  (10 equiv.) were calculated to be  $1.884 \times 10^{-2}$  and  $8.333 \times 10^{-3} \text{ mol L}^{-1}$ , respectively (Table S4, ESI†).

The mono-salicylidene Schiff base **NCL1** (Scheme 1) is not a stable compound in the solution-state. Unlike **CL1**, **NCL1** was observed to undergo hydrolysis of  $-N=CH-$  bond in  $\text{DMSO-d}_6$  (in the absence of any anion). Structural comparison of **NCL1** with **CL1** (Scheme 1) suggests that the two-electron withdrawing aromatic rings (benzonitrile and nitrophenol) attached to the imine bond possibly enhance the hydrolytic susceptibility of **NCL1** and facilitate  $-N=CH-$  bond cleavage in  $\text{DMSO-d}_6$  in the presence of hard-to-avoid traces of moisture adsorbed by the solvent. The presence of moisture ( $\text{H}_2\text{O}$ ) can be observed in the  $^1\text{H-NMR}$  spectrum of **NCL1** (at 3.36 ppm) which showed about 70% hydrolysis after 15 min. of sample preparation (Fig. S9, ESI†). The presence of moisture has also been detected in the  $^1\text{H-NMR}$  spectra of **SL**, **CL1** and **CL2** in  $\text{DMSO-d}_6$ , which indeed did not induce any hydrolysis of the salicylidene-based compounds under ambient conditions.

The bis-salicylidene Schiff base **NCL2** (Scheme 1) has previously been reported as a colorimetric fluoride sensor in  $\text{DMSO}$  using  $10^{-5} \text{ mol L}^{-1}$  solutions.<sup>9f</sup> However, **NCL2** is not sufficiently soluble in  $\text{DMSO-d}_6$  and other deuterated solvents ( $\text{CDCl}_3$ ,  $\text{CD}_3\text{CN}$  and  $\text{CD}_3\text{OD}$ ) to characterize the compound by NMR spectroscopy. We have observed that the addition of an excess of  $(n\text{-Bu}_4\text{N}^+)\text{F}^-$  or  $(n\text{-Bu}_4\text{N}^+)\text{H}_2\text{PO}_4^-$  (5 equiv.) resulted in complete solubilization of the compound in  $\text{DMSO-d}_6$ . **NCL2** was characterized in the presence of  $(n\text{-Bu}_4\text{N}^+)\text{H}_2\text{PO}_4^-$  where no immediate hydrolysis of  $-N=CH-$  bond was observed, and six peaks for six different sets of  $-CH$  protons in the aromatic region of the spectrum confirmed the purity of the compound (Fig. S8, ESI†). However, the salicylidene  $-OH$  peak could not be observed due to fast proton-exchange between phenolic  $-OH$  and  $\text{H}_2\text{PO}_4^-$  ions, as observed in the previous experiments. A solution of **NCL2** mixed with  $(n\text{-Bu}_4\text{N}^+)\text{F}^-$  in  $\text{DMSO-d}_6$  showed

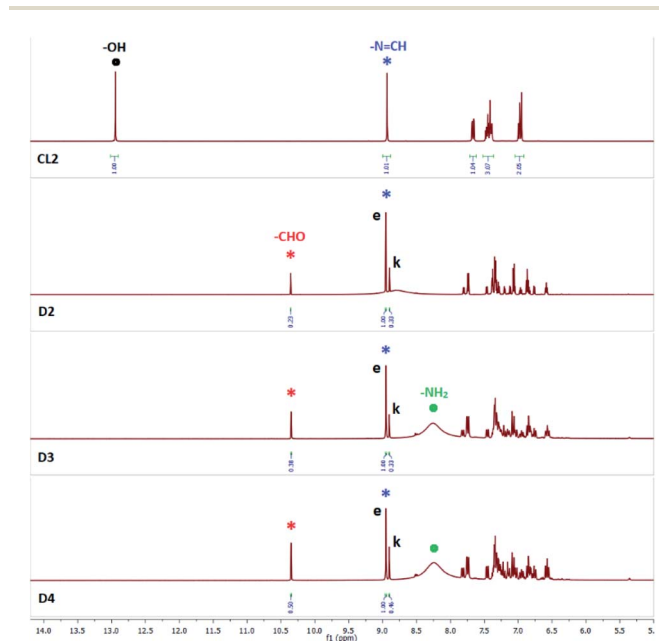


Fig. 6 Aromatic region of  $^1\text{H-NMR}$  spectra ( $\text{DMSO-d}_6$ ) of **CL2** in the presence of 5 equivalents of  $(n\text{-Bu}_4\text{N}^+)\text{H}_2\text{PO}_4^-$ , recorded after 24 hours (D2), 48 hours (D3) and after 72 hours (D4). Signals labelled with **e** and **k** indicate the enol and keto forms of **CL2** respectively. Signals labelled with red and blue asterisk indicate  $-CHO$  and  $-N=CH-$  peaks of salicylaldehyde (red) and **CL2** (blue) respectively. Signals labelled with black and green dots indicate  $-OH$  and  $-NH_2$  peaks of **CL2** (black) and amine product (green) respectively (additional spectra are provided in the ESI†).



about 35% hydrolysis after an hour and 47% hydrolysis was observed to be completed after 24 hours (Fig. S39, ESI†).

We have also carried out some  $^1\text{H}$ -NMR control experiments in order to validate the role of an anion in the hydrolysis of salicylidene Schiff bases. The following experiments are confirmative of the key role that anions play in the hydrolysis of salicylidene compounds in the presence of moisture. Addition of 15 equiv. of  $\text{H}_2\text{O}$  to a  $\text{DMSO}-d_6$  solution of **CL1** did not show any immediate hydrolysis of the compound in an hour, but showed 20% hydrolysis after 6 hours. The solution mixture when recorded after 24 hours showed 80% hydrolysis, and 95% hydrolysis was observed to be completed after 48 hours (Fig. S44, ESI†). Interestingly, addition of one equiv. of  $(n\text{-Bu}_4\text{N}^+)\text{Cl}^-$  to another  $\text{DMSO}-d_6$  solution of **CL1** containing 15 equiv. of  $\text{H}_2\text{O}$  showed complete hydrolysis of **CL1** within an hour (Fig. S43, ESI†). In contrast, 84% hydrolysis of **CL1** was observed to be completed after 24 hours in the presence of 5 equiv. of  $(n\text{-Bu}_4\text{N}^+)\text{Cl}^-$  in  $\text{DMSO}-d_6$  (Fig. 4). Similar experiments have also been performed with **CL2** and **SL**. Addition of 15 equiv. of  $\text{H}_2\text{O}$  to a  $\text{DMSO}-d_6$  solution of **CL2** showed only 18% and 26% hydrolysis after 24 and 72 hours respectively (Fig. 7). However, addition of one equiv. of  $(n\text{-Bu}_4\text{N}^+)\text{Cl}^-$  to another  $\text{DMSO}-d_6$  solution of **CL2** containing 15 equiv. of  $\text{H}_2\text{O}$  showed 45% and 71% hydrolysis after 24 and 72 hours respectively (Fig. 8). In a similar experiment, addition of one equiv. of  $(n\text{-Bu}_4\text{N}^+)\text{Cl}^-$  to a  $\text{DMSO}-d_6$  solution of **SL** containing 30 equiv. of  $\text{H}_2\text{O}$  showed 62% hydrolysis after 6 hours (Fig. S46, ESI†). Whereas, only 7% hydrolysis was completed for a solution of **SL** in  $\text{DMSO}-d_6$  containing 30 equiv. of  $\text{H}_2\text{O}$  after 6 hours (Fig. S45, ESI†). Further, splitting of the  $-\text{N}=\text{CH}-$  signals of **SL** and **CL2** have also been observed in the presence of water in  $\text{DMSO}-d_6$ , indicating that the hydrolysis proceeds *via* keto-enol tautomerism of salicylidene compounds. Thus, our control

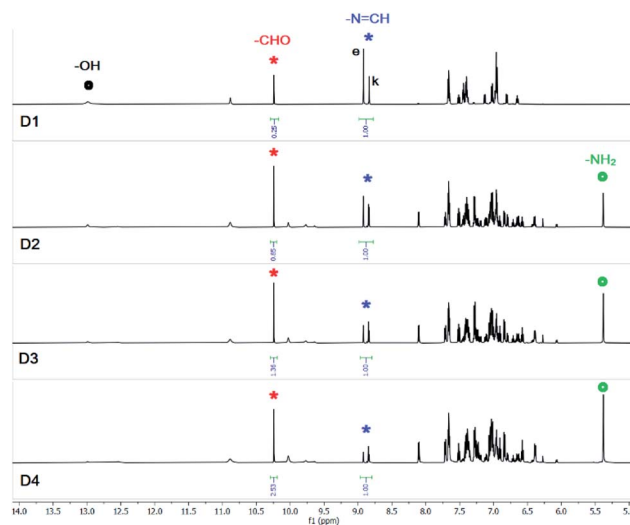


Fig. 8 Aromatic region of  $^1\text{H}$ -NMR spectra ( $\text{DMSO}-d_6$ ) of **CL2** in the presence of 15 equivalents of  $\text{H}_2\text{O}$  and 1 equivalent of  $(n\text{-Bu}_4\text{N}^+)\text{Cl}^-$ , recorded after 1 hour (D1), 24 hours (D2), 48 hours (D3) and after 72 hours (D4). Signals labelled with e and k indicate the enol and keto forms of **CL2** respectively. Signals labelled with red and blue asterisk indicate  $-\text{CHO}$  and  $-\text{N}=\text{CH}-$  peaks of salicylaldehyde (red) and **CL2** (blue) respectively. Signals labelled with black and green dots indicate  $-\text{OH}$  and  $-\text{NH}_2$  peaks of **CL2** (black) and amine product (green) respectively.

experiments suggest that the anions can significantly enhance the rate of hydrolysis in salicylidene compounds in moist solvent.

Based on the  $^1\text{H}$ -NMR experimental results, here we propose a plausible and general mechanism for anion-induced hydrolysis of salicylidene Schiff bases in the presence of moisture (Scheme 2). In the first step, the salicylidene  $-\text{OH}$  group which is involved in intramolecular hydrogen bonding with imine nitrogen (A in Scheme 2), forms an  $\text{O}-\text{H}\cdots\text{A}^-$  hydrogen bonded complex (B in Scheme 2).<sup>16</sup> The fact that the peak position of the salicylidene  $-\text{OH}$  proton in **SL** did not shift upon addition of halides ( $\text{Cl}^-$  and  $\text{Br}^-$ ) suggest that the intramolecular  $\text{O}-\text{H}\cdots\text{N}$  hydrogen bond persists in the presence of these anions. However, broadening or disappearance of the salicylidene  $-\text{OH}$  peak in the presence of anions can be attributed to proton-exchange processes in the solution-state. In the second step, the hydrogen bonded enol form (B in Scheme 2) can partly tautomerize to the hydrogen bonded keto form (D in Scheme 2) *via* a transient zwitterion form (C in Scheme 2).<sup>11</sup> Splitting of the  $-\text{N}=\text{CH}-$  peak (at 8.9/9.0 ppm) into two closely spaced signals were observed in the  $^1\text{H}$ -NMR experiments of **SL** and **CL2** in the presence of anions, indicating the presence of both enol and keto forms.<sup>10</sup> The proton-exchange processes possibly facilitate the keto-enol tautomerism in the presence of anions, which was also observed in the  $^1\text{H}$ -NMR spectra of **SL** and **CL2** in the presence of water (see ESI†). In the next step, moisture present in the  $\text{DMSO}-d_6$  solution mixture can behave as a nucleophile and attack on the imine carbon of the hydrogen bonded enol form (B) or the keto form (D) to generate a hydrogen bonded intermediate of hydroxy(phenylamino)methyl phenol (E in

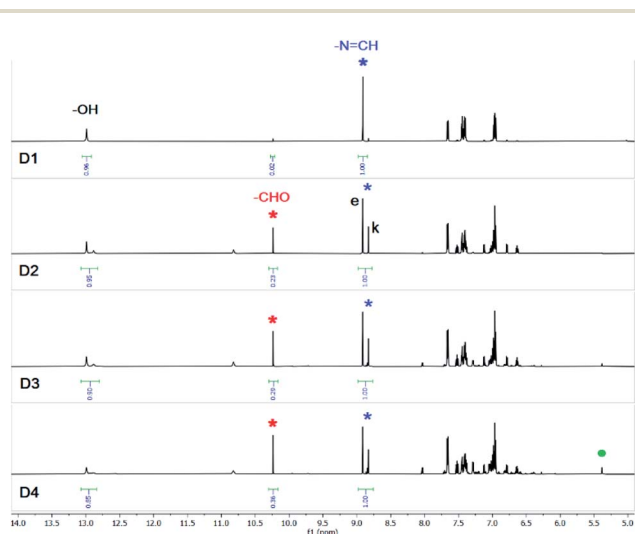


Fig. 7 Aromatic region of  $^1\text{H}$ -NMR spectra ( $\text{DMSO}-d_6$ ) of **CL2** in the presence of 15 equivalents of  $\text{H}_2\text{O}$ , recorded after 1 hour (D1), 24 hours (D2), 48 hours (D3) and after 72 hours (D4). Signals labelled with e and k indicate the enol and keto forms of **CL2** respectively. Signals labelled with red and blue asterisk indicate  $-\text{CHO}$  and  $-\text{N}=\text{CH}-$  peaks of salicylaldehyde (red) and **CL2** (blue) respectively.





Scheme 2). Due to the acidic nature of phenolic –OH and the presence of a nearby –NH group, intermediate form E may possibly exist in an equilibrium with the zwitterionic form F, similar to B and C. As anions are present in excess in the solution, it is very likely that both the –NH and –OH protons will engage in hydrogen bonding with anions. The participation of the amine –NH proton in hydrogen bonding with an anion has also been observed in the  $^1\text{H-NMR}$  experiments, where down-field shift (with or without concomitant broadening) of –NH peak was observed as hydrolysis progressed. Finally, formation of the C=O double bond by the loss of the O–H proton in E or F results in the cleavage of the HC–NH bond to generate salicylaldehyde and respective aromatic amine (G and H in Scheme 2). Depending upon the basicity of the anion, the regenerated salicylaldehyde can either exist in its neutral form, where the –OH group will be hydrogen bonded to the anion (H in Scheme 2) or in its deprotonated phenolate form.

However, we are also having the opinion that based on a specific anion under investigation, the mechanism of –N=CH– bond hydrolysis may somewhat vary.

It is important to mention again that, both DMSO- $d_6$  and some tetrabutylammonium salts used in the  $^1\text{H-NMR}$  experiments are hygroscopic in nature, and it is always difficult to avoid the presence of moisture in the prepared samples under ambient conditions. All experiments performed in the reported literatures were under ambient conditions, and no mention has been made that the experiments were carried out under inert conditions.<sup>7,8</sup>

## Conclusion

In conclusion, we have proven that the salicylidene Schiff bases (**SL**, **CL1** and **CL2**) undergo gradual hydrolysis of imine bonds in the presence of tetrabutylammonium salts of halides and oxo-anions in moist aprotic solvent. Bromide and hydrogensulfate ions were observed to show minimal effect on the hydrolysis of the tris-salicylidene compound **SL** due to the presence of multiple imine bonds and weakly basic nature of these anions having low hydration enthalpy. The extent of hydrolysis in the salicylidene Schiff bases is largely dependent on the structure of the receptor (number of imine bonds), quantity of anions ( $n\text{-Bu}_4\text{N}^+$  salts) used in the NMR experiments and moisture adsorbed by the DMSO- $d_6$  solution mixture containing ( $n\text{-Bu}_4\text{N}^+$ ) $\text{X}^-$ .

Formation of the receptor–anion hydrogen bonded complex and subsequent keto–enol tautomerism could clearly be observed in the  $^1\text{H-NMR}$  experiments of **CL2** mixed with ( $n\text{-Bu}_4\text{N}^+$ ) $\text{X}^-$  salts of halides (chloride/bromide) and oxo-anions. Similar to **CL2**, splitting of the –N=CH– peak has also been observed in the  $^1\text{H-NMR}$  experiments of **SL** in the presence of chloride, acetate and dihydrogenphosphate ions (although less prominent), suggesting the presence of both keto and enol tautomers of **SL** in solution. The mono-salicylidene compound **CL1** undergoes much faster anion-induced hydrolysis as compared to **CL2** and **SL**, and no keto–enol tautomerism was observed in the case of **CL1**.

Thus, due to the apparently unavoidable hydrolysis of the salicylidene Schiff bases in the presence of anions under ambient conditions, it is of utmost concern to validate the solution-state stability of Schiff bases prior to anion sensing studies. Overall, our experimental results demonstrate the limitations of the salicylidene Schiff bases as anion sensors, and suggests a plausible mechanism for the anion-induced hydrolysis of –N=CH– bonds *via* receptor–anion hydrogen bonding and keto–enol tautomerism based on  $^1\text{H-NMR}$  studies.

## Conflicts of interest

There are no conflicts to declare.

## Acknowledgements

SKD acknowledges the Department of Science and Technology (DST), New Delhi, India for providing financial support through INSPIRE Faculty award (DST/INSPIRE/04/2016/001867). SKD and CJ thank the Alexander von Humboldt Foundation, Bonn, Germany for providing the opportunity for research collaboration. We thank Mrs Birgit Tommes for her great help in obtaining the NMR spectra at HHU Dusseldorf.

## Notes and references

- (a) X. Liu and J.-R. Hamon, *Coord. Chem. Rev.*, 2019, **389**, 94–118; (b) M. Karmakar and S. Chattopadhyay, *J. Mol. Struct.*, 2019, **1186**, 155–186; (c) J. Zhang, L. Xu and W.-Y. Wong, *Coord. Chem. Rev.*, 2018, **355**, 180–198; (d) C. M. da Silva, D. L. da Silva, L. V. Modolo, R. B. Alves, M. A. de Resende, C. V. B. Martins and A. de Fátima, *J. Adv. Res.*, 2011, **2**, 1–8; (e) M. Nath and P. K. Saini, *Dalton Trans.*, 2011, **40**, 7077–7121; (f) W. A. Zoubi, S. G. Mohamed, A. A. S. Al-Hamdani, A. P. Mahendradhany and Y. G. Ko, *RSC Adv.*, 2018, **8**, 23294–23318.
- (a) P. G. Cozzi, *Chem. Soc. Rev.*, 2004, **33**, 410–421, and references therein; (b) K. C. Gupta and A. C. Sutar, *Coord. Chem. Rev.*, 2008, **252**, 1420–1450; (c) R. Drozdak, B. Allaert, N. Ledoux, I. Dragutan, V. Dragutan and F. Verpoort, *Adv. Synth. Catal.*, 2005, **347**, 1721–1743; (d) P. Adao, M. L. Kuznetsov, S. Barroso, A. M. Martins, F. Avecilla and J. C. Pessoa, *Inorg. Chem.*, 2012, **51**, 11430–11449; (e) P. Das and W. Linert, *Coord. Chem. Rev.*, 2016, **311**, 1–23; (f) D. Gong, B. Wang, X. Jia and X. Zhang, *Dalton Trans.*, 2014, **43**, 4169–4178.
- (a) C. M. Che, S. C. Chan, H. F. Xiang, M. C. Chan, Y. Liu and Y. Wang, *Chem. Commun.*, 2004, 1484–1485; (b) T. Sano, Y. Nishio, Y. Hamada, H. Takahashi, T. Usuki and K. Shibata, *J. Mater. Chem.*, 2000, **10**, 157–161; (c) S. H. Li, F. R. Chen, Y. F. Zhou, J. N. Wang, H. Zhang and J. G. Xu, *Chem. Commun.*, 2009, 4179–4181; (d) S. A. Lee, G. R. You, Y. W. Choi, H. Y. Jo, A. R. Kim, I. Noh, S. J. Kim, Y. Kim and C. Kim, *Dalton Trans.*, 2014, **43**, 6650–6659.
- (a) Y. Sun, Y. Lu, M. Bian, Z. Yang, X. Ma and W. Liu, *Eur. J. Med. Chem.*, 2021, **211**, 113098; (b) S. Parveen, *Appl. Organomet. Chem.*, 2020, **34**, e5687; (c) M. S. More,





- P. G. Joshi, Y. K. Mishra and P. K. Khanna, *Mater. Today Chem.*, 2019, **14**, 100195; (d) M. T. Kaczmarek, M. Zabiszak, M. Nowak and R. Jastrzab, *Coord. Chem. Rev.*, 2018, **370**, 42–54; (e) M. Hajrezaie, M. Paydar, C. Y. Looi, S. Z. Moghadamtousi, P. Hassandarvish, M. S. Salga, H. Karimian, K. Shams, M. Zahedifard, N. A. Majid, H. M. Ali and M. A. Abdulla, *Sci. Rep.*, 2015, **5**, 9097–9104.
- 5 K. Bowman-James, A. Bianchi and E. Garcia-Espana, *Anion Coordination Chemistry*, Wiley-VCH, 1st edn, 2011.
- 6 J. W. Steed and J. L. Atwood, *Supramolecular Chemistry*, Wiley, New York, 2nd edn, 2000.
- 7 (a) R. Sivakumar, V. Reena, N. Ananthi, M. Babu, S. Anandan and S. Velmathi, *Spectrochim. Acta, Part A*, 2010, **75**, 1146–1151; (b) A. Bhattacharyya, S. C. Makhal, S. Ghosh and N. Guchhait, *Spectrochim. Acta, Part A*, 2018, **198**, 107–114; (c) J. Li, H. Lin, Z. Cai and H. Lin, *Spectrochim. Acta, Part A*, 2009, **72**, 1062–1065; (d) K. Liu, X. Zhao, Q. Liu, J. Huo, H. Fu and Y. Wang, *J. Photochem. Photobiol., B*, 2014, **138**, 75–79; (e) Q. Li, Y. Guo, J. Xu and S. Shao, *Sens. Actuators, B*, 2011, **158**, 427–431; (f) R. Arabahmadi, M. Orojloob and S. Amani, *Anal. Methods*, 2014, **6**, 7384–7393.
- 8 (a) D. Sharma, R. K. Bera and S. K. Sahoo, *Spectrochim. Acta, Part A*, 2013, **105**, 477–482; (b) L. Zang and S. Jiang, *Spectrochim. Acta, Part A*, 2015, **150**, 814–820; (c) S. Dalapati, S. Jana and N. Guchhait, *Spectrochim. Acta, Part A*, 2014, **129**, 499–508; (d) S. Suganya and S. Velmathi, *J. Mol. Recognit.*, 2013, **26**, 259–267; (e) P. Alreja and N. Kaur, *Inorg. Chim. Acta*, 2018, **480**, 127–131; (f) Y. Hijji and G. Wairia, *Proc. SPIE*, 2005, 60070B; (g) Y. M. Hijji, B. Bararea, A. P. Kennedy and R. Butcher, *Sens. Actuators, B*, 2009, **136**, 297–302; (h) S. Daniel, *Bull. Mater. Sci.*, 2020, **43**, 157; (i) N. Yildirim and M. Yildiz, *J. Turk. Chem. Soc., Sect. A*, 2018, **5**, 1271–1278; (j) S. Dalapati, M. A. Alam, S. Jana and N. Guchhait, *J. Fluorine Chem.*, 2011, **132**, 536–540; (k) X. Huang, Y. He, Z. Chen and C. Hu, *Chin. J. Chem.*, 2009, **27**, 1526–1530; (l) V. Reena, S. Suganya and S. Velmathi, *J. Fluorine Chem.*, 2013, **153**, 89–95.
- 9 E. A. Katayev, Y. A. Ustynyuk and J. L. Sessler, *Coord. Chem. Rev.*, 2006, **250**, 3004–3037.
- 10 S. K. Dey and C. Janiak, *RSC Adv.*, 2020, **10**, 14689–14693.
- 11 (a) M. Enamullah, A.-C. Chamayou, K. S. Banu, A. C. Kautz and C. Janiak, *Inorg. Chim. Acta*, 2017, **464**, 186–194; (b) B. M. Drašković, G. A. Bogdanović, M. A. Neelakantan, A.-C. Chamayou, S. Thalamuthu, Y. S. Avadhut, J. Schmedt auf der Gönne, S. Banerjee and C. Janiak, *Cryst. Growth Des.*, 2010, **10**, 1665–1676.
- 12 L. Wang, L. Yang and D. Cao, *J. Fluoresc.*, 2014, **24**, 1347–1355.
- 13 (a) Y. Sun, Y. Liu and W. Guo, *Sens. Actuators, B*, 2009, **143**, 171–176; (b) S. K. Padhana, M. B. Podha, P. K. Sahub and S. N. Sahu, *Sens. Actuators, B*, 2018, **255**, 1376–1390; (c) T. M. Asha, E. Shiju, C. Keloth and M. R. P. Kurup, *Appl. Organomet. Chem.*, 2020, e5520; (d) F. Wang, L. Wang, X. Chen and J. Yoon, *Chem. Soc. Rev.*, 2014, **43**, 4312–4324; (e) Y. Ding, T. Li, W. Zhu and Y. Xie, *Org. Biomol. Chem.*, 2012, **10**, 4201–4207; (f) P. R. Lakshmi, R. Manivannan, P. Jayasudha and K. P. Elango, *Anal. Methods*, 2018, **10**, 2368–2375; (g) Z. Xu, X. Chen, H. N. Kim and J. Yoon, *Chem. Soc. Rev.*, 2010, **39**, 127–137.
- 14 (a) J. Cao, C. Zhao, P. Feng, Y. Zhang and W. Zhu, *RSC Adv.*, 2012, **2**, 418–420; (b) S. Yang, Y. Liu and G. Feng, *RSC Adv.*, 2013, **3**, 20171–20178; (c) S. Xu, K. Chen and H. Tian, *J. Mater. Chem.*, 2005, **15**, 2676–2680; (d) B. Zhu, F. Yuan, R. Li, Y. Li, Q. Wei, Z. Ma, B. Du and X. Zhang, *Chem. Commun.*, 2011, **47**, 7098–7100; (e) P. Chen, W. Bai and Y. Bao, *J. Mater. Chem. C*, 2019, **7**, 11731–11746; (f) L. Fu, F.-L. Jiang, D. Fortin, P. D. Harvey and Y. Liu, *Chem. Commun.*, 2011, **47**, 5503–5505; (g) Shweta, A. Kumar, Neeraj, S. K. Asthana and K. K. Upadhyay, *New J. Chem.*, 2017, **41**, 5098–5104; (h) J. Chen, C. Liu, J. Zhang, W. Ding, M. Zhou and F. Wu, *Chem. Commun.*, 2013, **49**, 10814–10816; (i) B. Li, C. Zhang, C. Liu, J. Chen, X. Wang, Z. Liu and F. Yi, *RSC Adv.*, 2014, **4**, 46016–46019.
- 15 (a) S. K. Dey and G. Das, *Dalton Trans.*, 2011, **40**, 12048–12051; (b) N. Busschaert, M. Wenzel, M. E. Light, P. Iglesias-Hernandez, R. Perez-Tomas and P. A. Gale, *J. Am. Chem. Soc.*, 2011, **133**, 14136–14145; (c) A. Basu, S. K. Dey and G. Das, *RSC Adv.*, 2013, **3**, 6596–6605; (d) M. E. Khansari, M. H. Hasan, C. R. Johnson, N. A. Williams, B. M. Wong, D. R. Powell, R. Tandon and M. A. Hossain, *ACS Omega*, 2017, **2**, 9057–9066; (e) S. K. Dey, Archana, S. Pereira, S. S. Harmalkar, S. N. Mhalidar, V. V. Gobre and C. Janiak, *CrystEngComm*, 2020, **22**, 6152–6160.
- 16 S. K. Patil and D. Das, *ChemistrySelect*, 2017, **2**, 6178–6186.

